

Newer concepts in neural anatomy and neurovascular preservation in robotic radical prostatectomy

Sailaja Pisipati, Adnan Ali, Rao S. Mandalapu, George K. Haines III¹, Paras Singhal, Balaji N. Reddy, Robert Leung, Ashutosh K. Tewari

Departments of Urology and ¹Pathology, Icahn School of Medicine, Mount Sinai Hospital, New York, NY 10029, USA

ABSTRACT

With more than 60% of radical prostatectomies being performed robotically, robotic-assisted laparoscopic prostatectomy (RALP) has largely replaced the open and laparoscopic approaches and has become the standard of care surgical treatment option for localized prostate cancer in the United States. Accomplishing negative surgical margins while preserving functional outcomes of sexual function and continence play a significant role in determining the success of surgical intervention, particularly since the advent of nerve-sparing (NS) robotic prostatectomy. Recent evidence suggests that NS surgery improves continence in addition to sexual function. In this review, we describe the neuroanatomical concepts and recent developments in the NS technique of RALP with a view to improving the “trifecta” outcomes.

Key words: Prostatic neuroanatomy, nerve sparing, robotic assisted laparoscopic prostatectomy

INTRODUCTION

The introduction of prostate-specific antigen (PSA) screening over the last two decades has resulted in stage migration of prostate cancer.^[1] Radical prostatectomy (RP) for organ-confined prostate cancer is an effective treatment option but can result in erectile dysfunction (ED) and incontinence in a significant proportion of patients. The reported rates of post-operative potency vary widely from 21% to 86%.^[2] The prevalence of urinary incontinence following RALP ranges from 4% to 31%.^[3] With an increasing number of men being diagnosed at a younger age, achieving the “trifecta goals” is of utmost importance to improving the quality of life. Accomplishing negative surgical margins while

preserving functional outcomes of sexual function and continence plays a significant role in determining the success of surgical intervention, particularly since the advent of nerve sparing (NS) RP. With more than 60% of RP being performed robotically, robot-assisted laparoscopic prostatectomy (RALP) has largely replaced the standard open radical prostatectomy (ORP) and laparoscopic radical prostatectomy (LRP) as a surgical treatment option for prostate cancer.^[4] A meta-analysis by Tewari *et al.* in 2012 has demonstrated that margin rates are comparable between RALP and ORP, with LRP demonstrating an increased risk for positive surgical margins (PSM). The meta-analysis also revealed that the robotic approach is the safest in terms of perioperative complications.^[5] Recent evidence suggests that NS not only improves sexual function but also enhances continence recovery.^[6,7] It is in the pursuit of these improved oncological outcomes along with preservation of sexual function and continence that RALP can have the greatest impact. In this review, we describe the neuroanatomical concepts and recent developments in the NS technique of RALP with a view to improving the “trifecta” outcomes.

For correspondence: Dr. Ashutosh K. Tewari,
Department of Urology, The Carroll and Milton Petrie
Foundation, Icahn School of Medicine at Mount Sinai,
1425 Madison Avenue, L6-50, New York, NY 10029, USA.
E-mail: ashtewari@mountsinai.org

Access this article online	
Quick Response Code:	Website: www.indianjurol.com
	DOI: 10.4103/0970-1591.142064

Prostatic neuro-anatomy re-visited

The pioneering contributions of Walsh *et al.* in 1982 on the anatomic dissection for preservation of the neurovascular bundles (NVBs) remains one of the most significant landmarks in urological history.^[8] It is well known that autonomic nerves contribute to penile erection. The inferior hypogastric plexus, comprised of the sympathetic fibers from T11-L2 ganglia and the parasympathetics from the ventral rami of

S2-S4 spinal nerves, sends efferents to the pelvic viscera. The parasympathetics from this plexus situated behind the rectum travel past the seminal vesicles and along the posterolateral aspect of the prostate and descend posterior and lateral to the urethra before they penetrate the urogenital diaphragm to continue posterior to the dorsal penile artery.^[8] Because of the reversal of steps of RP with the robotic approach and the advantages of RALP that include seven degrees of freedom, improved ergonomics and three-dimensional vision, the anatomical foundations of the neuronal architecture were re-visited by Tewari *et al.*^[9] The course of the NVBs from its origin in the pelvic plexus down to its course along the urethra using the minimally invasive approach was studied using cadaveric models.^[9] The NVBs were found to be situated typically in an anterolateral location, but were found to occupy the posterolateral aspect on rare occasions.^[10,11] Tewari *et al.* described that this network of interconnecting neural fibers around the prostate and seminal vesicles was arranged as a hammock in a trizonal distribution.^[12] Takenaka *et al.* described the fan-like distribution of the parasympathetic fibers lying about 2 cm distal to the prostatic-vesical junction on the posterolateral aspect of the prostate.^[13] Takenaka and Tewari *et al.* have also demonstrated the presence and the distribution of the autonomic ganglion cells in the pelvic plexus and around the bladder and the prostate.^[9,14] Additionally, the NVBs were found to be occupying a potential avascular triangular space bounded by the anterior layer of the Denonvillier's fascia posteriorly, prostatic fascia medially and the lateral pelvic fascia laterally.^[9] Additional erectile nerves in the "Veil of Aphrodite" along the anterolateral aspect of the prostate were identified by Menon and colleagues.^[11] Costello *et al.* identified that the array of nerve fibers coursing along the posterolateral aspect of the prostate inferior to the tip of the seminal vesicles formed a more well-defined bundle at the mid-prostatic position before re-diverging near the apex.^[15] According to another report, a reasonable amount of nerves were identified on the ventral aspect of the prostate in addition to the classical posterolateral location.^[16]

Trizonal neural architecture

The "trizonal" neural architecture is comprised of the proximal neurovascular plate (PNP), predominant neurovascular bundle (PNB) and accessory neural pathways (ANP) arranged around the prostate as a neural hammock [Figure 1].^[12,13]

The PNP is situated lateral to the bladder neck and seminal vesicles (SV) and is intermingled with branches of the inferior vesical vasculature. It is located 5 mm lateral to the SV, within 6 mm of the bladder neck, 5 mm of the endopelvic fascia and overlaps 5 mm of the prostate. It measures 3 mm thick, 7 mm wide and 9 mm long. It is the integrating center for the processing and relaying of erectogenic neural impulses and is prone to injury during incision of the endopelvic fascia, incision of the prostatic-vesical junction, lateral dissection of the SV, application of a bulldog clamp and division of prostatic pedicles.^[12]

Enclosed within the layers of the levator fascia and/or lateral pelvic fascia and within the groove between the prostate and the rectum lies the PNB, which carries neural impulses to the erectile tissue and exhibits a variable course, shape and size. The PNB was thickest at the base, and was most variable in course and architecture near the apex. In 66% of the cases, a medial extension was noted behind the prostate, which converged medially at the apex in 33% of the cases. The ganglion cells in the PNB are attached to the prostatic capsule or embedded within the capsule; hence, the need for cautious, athermal dissection to avoid injury.^[12] PNBs are prone to injury during the dissection of endopelvic fascia, controlling the pedicles, during release of NVBs, apical transection and urethral anastomosis.

ANPs are putative accessory neural pathways within the layers of levator and/or lateral pelvic fascia, on the anterolateral (42%) and occasionally on the posterolateral aspect of the prostate (25%). ANPs may be damaged during dissection of the endopelvic fascia, suturing the dorsal venous complex while applying back-bleeding suture during posterior dissection, controlling the pedicle, release of NVBs, during apical transection or while performing urethral anastomosis.^[12]

The steps of RALP during which each of these trizonal neural structures are likely to be injured and the preventive measures to be taken to avoid such injury have been previously described by Tewari *et al.*^[12] Establishing a clear anatomical map of the neurovascular structures related to RALP has empowered surgeons with the knowledge to enhance their NS technique, which is crucial for functional recovery.

Techniques to preserve NVB

The majority of the fibers of the NVBs lie in between the prostatic fascia (medial layer of the lateral pelvic fascia) and the levator fascia (lateral layer of the lateral pelvic fascia). The venous/vascular layer acts as a landmark during NS surgery. Various terminologies have been coined to describe the incisions through the planes around the prostate during NS RALP.

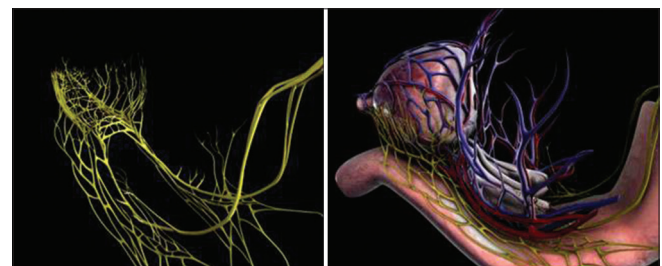


Figure 1: The trizonal neural network comprising of the proximal neurovascular plate (PNP), the predominant neurovascular bundles (PNB) and accessory neural pathways (ANP) form a neural hammock around the prostate. Medical animation representing the neural hammock

The veil of Aphrodite technique proposed by Menon involves anterior incision of the prostatic fascia to enter the plane between the prostatic capsule and the prostatic fascia. This follows the posterior and the posterolateral dissection in the plane between the prostatic fascia and the Denonvillier's fascia. The periprostatic tissue hanging from the bladder neck down toward the urethro-apical junction is known as the "Veil of Aphrodite."^[17] The technique was refined in 2009, in which the anterior prostatic fascial tissue, adherent to the capsule, dorsal venous complex and the pubovesical ligaments, was preserved. Adopting this modification known as the "superveil" technique, it was believed that the nerves interposed between the 11-o' clock and the 1-o' clock positions were preserved.^[18]

Another conventional nomenclature used for the NS approach is the intrafascial, interfascial and extrafascial approach [Table 1]. However, this classification system is slowly being replaced by the graded NS approach.

We now routinely adopt the athermal, traction-free, risk-stratified graded NS approach described below to optimize our oncological and functional outcomes.

Athermal technique

Various modifications have been made to the technique of NS RALP over the last decade. In an attempt to minimize thermal and ischemic damage to the delicate neurovascular tissues, Tewari *et al.* introduced the concept of "Athermal Robotic technique" (ART) in 2005.^[19] Based on the understanding of the trizonal neural anatomy and by adopting the ART, 45% sexual function was achieved at 6 weeks.^[20] Technical feasibility of the athermal technique has been proven even in large prostates.^[21] In a study of 215 patients who had RALP, 87% of those who had bilateral NS, are <70 years and were

pre-operatively potent, were potent at 1 year following surgery. The overall PSM rate was 6.5%.^[22]

In a study comparing monopolar cautery, bipolar cautery and a cautery-free technique, Ahlering *et al.* noticed nearly a five-fold improvement of potency recovery at 3 and 9 months with the cautery-free approach.^[23] A cumulative analysis of eight studies in a systematic review by Ficarra *et al.* revealed better potency outcomes with the athermal NS technique at 3, 6 and 12 months.^[24] It is hence believed that avoiding/minimizing thermal energy, particularly while dissecting the NVBs, results in better functional outcomes.

Traction-Free technique

Another modification adopted to the NS technique is a traction-free approach.^[19] Undue stretch on the NVB causes mechanical trauma resulting in axonotemesis and disruption of the vasa nervorum thus resulting in neural and vascular insults. In addition, tissue hypoxia can result due to injury to the accessory pudendal arteries that run along the anterolateral surface of the bladder and the prostate in 70% of the cases.^[25] Such vascular insults account for hypoxia, nutrient deficiency, free radical formation and accumulation of neurotoxic elements that result in ischemia and delayed recovery. It is hypothesized that reducing or avoiding traction on the NVB minimizes the chances of stretch-induced axonotemesis and tissue hypoxia thus resulting in better functional outcomes. The lack of tactile feedback in robotic surgery poses a challenge in detecting excessive traction placed on the neurovasculature during the procedure. In an attempt to overcome this drawback, Tewari *et al.* developed the concept of real-time intraoperative penile oxygenation monitoring as a surrogate for identifying traction. This involved the use of an auditory probe that provided feedback in the form of an alarm when the tissue oxygenation dropped below 85%. Subtle, deliberate modifications to certain steps during the procedure, based on this auditory feedback, resulted in maintenance of penile oxygenation at or above 85% during the surgery.^[26] Using this device, Tewari *et al.* reported that a significantly higher proportion of patients with bilateral NS in the study group had no ED when compared with the control group at 6 and 52 weeks post-RALP. 93.9% and 78.4% of patients in the study and control groups, respectively, had a SHIM score ≥ 17 at 1 year. The overall PSM rates in the study and control groups were 9.4% and 9.9%, respectively. Feedback obtained by real-time tissue oxygen monitoring has allowed subtle technical adjustments thus amounting to improved functional outcomes.

Risk-stratified graded NS

The concept of graded NS approach to improve sexual outcomes was introduced in 2008.^[27] In an attempt to balance the competing goals of oncological cure and sexual recovery, a "novel" risk stratification strategy has been proposed^[28,29] [Figures 2-4] [Table 2]. Based on several

Table 1: Intrafascial, interfascial and extrafascial approach

Approach	Description of incision	Periprostatic tissue on the excised specimen
Extrafascial (non-NS)	Incision is taken along the lateral aspect of the levator fascia/lateral layer of the lateral pelvic fascia, close to the levator ani	Large amount-prostatic capsule, prostatic fascia, levator fascia, Denonvillier's fascia
Interfascial (partial NS)	Incision is taken lateral to the prostatic fascia at the anterolateral and the posterolateral aspects of the prostate	Moderate amount-prostatic capsule, prostatic fascia and Denonvillier's fascia
Intrafascial (complete NS)	Incision is taken between the prostatic capsule and the prostatic fascia along the anterolateral and posterolateral aspects of the prostate and anterior to the Denonvillier's fascia on the posterior aspect	Minimal amount-prostatic capsule, no periprostatic tissue, small amount of Denonvillier's fascia might be present in the midline posteriorly

NS=Nerve-sparing

pre-operative parameters including PSA, clinical stage, Gleason grade on biopsy and pre-operative magnetic resonance imaging (MRI) findings, patients are categorized into one of four risk grades, where risk grade 1 patients receive NS grade 1 and so on for risk grades 2-4. By adopting this risk-stratified approach for neural hammock preservation during RALP, Tewari *et al.* were able to improve potency outcomes without compromising oncological outcomes in a cohort of 1263 patients. The authors reported higher

rates of intercourse (90.9% and 62% for grades 1 and 4 NS, respectively) and return to baseline sexual function (81.7% and 54.4% for grades 1 and 4, respectively) in patients who had greater degrees (lower grades) of NS. The overall PSM rates for patients with NS grades 1, 2, 3 and 4 were 9.9%, 8.1%, 7.2% and 8.7%, respectively ($P = 0.64$). With increasing degree of NS, PSM rates were not significantly elevated; potency outcomes, however, were significantly better.^[30]

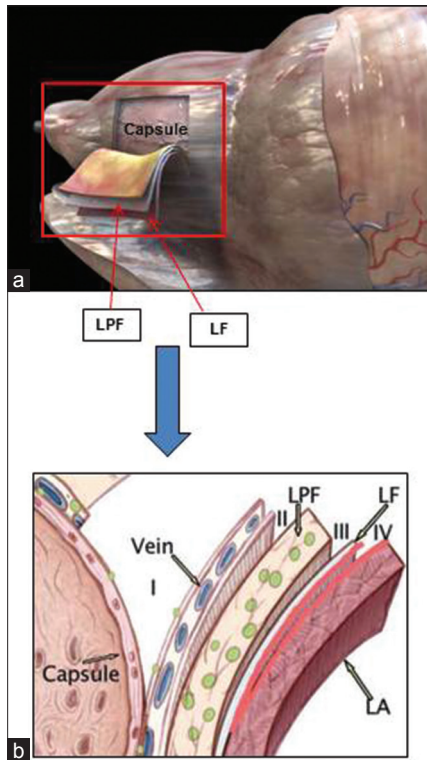


Figure 2: Planes of dissection for nerve sparing grades 1–4. (a) Medical animation. (b) Diagrammatic representation of the layers of fascia enveloping the prostatic capsule, showing the planes of dissection. LPF = lateral pelvic fascia medial layer, i.e., prostatic fascia; LF = lateral pelvic fascia lateral layer, i.e., levator fascia; LA = levator ani. B – Reproduced with permission from [24]

Schatloff *et al* described a five-point NS grading system based on intraoperative visual cues. According to their system, a non-NS procedure was assigned grade 1 and the best NS ($\geq 95\%$) was graded as 5, with $<50\%$, 50% and 75% NS being coded as grades 2, 3 and 4, respectively.^[31] According to a subjective model of a four-point NS score (NSS) grading system proposed by Moskovic *et al.*, where NSS 1 meant complete preservation (i.e. full NS) and 4 was complete resection (i.e. non-NS), a lower NSS was one of the independent predictors of sexual function recovery at 24 months.^[32]

Available data support the fact that cavernosal preservation during RALP is no longer an “all or none” phenomenon, but

Table 2: Grades of nerve sparing robotic radical prostatectomy

Grades of NS	Description of incision
1 (Complete NS)	Incision of the Denonvilliers’ and lateral pelvic fascia just outside the prostatic capsule. Highest degree of NS possible
2	Incision through Denonvilliers’ and LPF just outside the layers of veins of prostatic capsule
3 (Incremental NS)	Incision through the outer compartment of the LPF, excising all layers of Denonvilliers’ fascia. Partial/moderate degree of NS
4 (Non-NS)	Wide excision of LPF and Denonvilliers’ fascia. Least degree of NS possible/non-NS

NS=Nerve-sparing, LPF=Lateral pelvic fascia

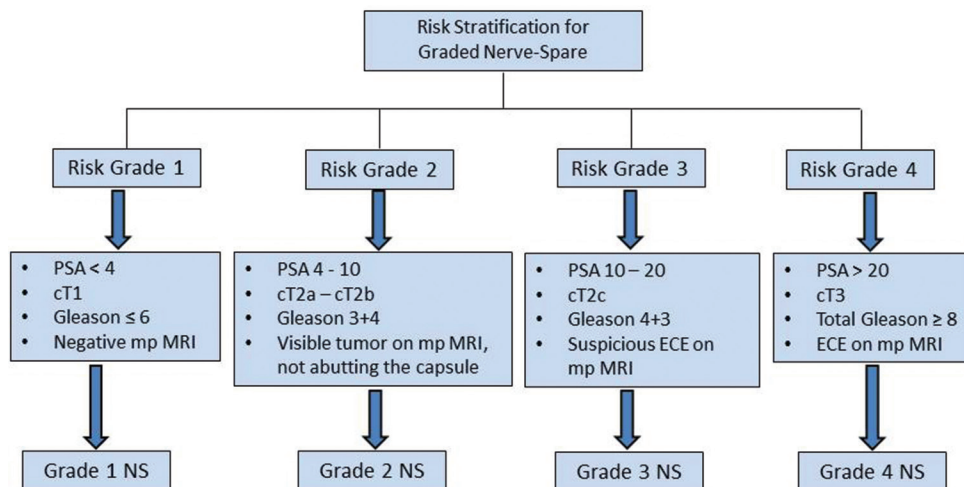


Figure 3: Risk stratification algorithm for athermal nerve sparing robotic radical prostatectomy. (ECE = extracapsular extension; mp MRI = multiparametric magnetic resonance imaging)

is a graded entity. The grading system enables the surgeon to achieve better “trifecta” outcomes.

Intra-operative frozen sections

RP involves interplay between competing goals of cancer extirpation, NS, post-operative recovery of urinary continence and potency. This requires precise dissection in an appropriate plane to achieve effective cancer control by avoiding PSMs and performing adequate NS concurrently. At present, there is no consensus on the use of frozen sections during RP. Various studies have gauged the utility of intraoperative frozen section analysis performed at different sites of the prostate/periprostatic soft tissue, and the results vary widely. This variation is mostly due to differences in sampling methods (sites or whole margins) and sites. Neurovascular structure–adjacent frozen section examination (NeuroSAFE) technique of intraoperative frozen section (IFS) analysis allows real-time histological evaluation and helps in performing a NS procedure without compromising oncological safety. Schlomm *et al.* demonstrated in a cohort of 11,069 patients a feasible intraoperative technique of NeuroSAFE.^[33] This technique

enables real-time histologic monitoring of the oncologic safety of an NS procedure. Systematic NeuroSAFE was reported to significantly increase NS frequency and reduces PSMs. Also, patients with a NeuroSAFE-detected PSM were converted to a prognostically more favorable NSM status by secondary wide resection. In this study, a false-negative IFS result was reported in 2.5% of the cases. In this context, our group is currently developing an MRI-guided intraoperative frozen section technique [Figure 5]. The preliminary results will be available in the near future.

Imaging and nerve mapping techniques to identify the NVB Localization by imaging modalities

Infiltration of the neoplastic cells around the cavernosal nerve fibers and extraprostatic extension are microscopic phenomena that cannot be visualized intraoperatively even with the x10-12 magnification of the stereoscope of the daVinci system. The inability to identify malignant cells and their association with nerves can result in incomplete removal of the cancerous tissue resulting in PSM, post-operative impotence due to damage to/excision of the cavernous nerves or a combination of both. In order

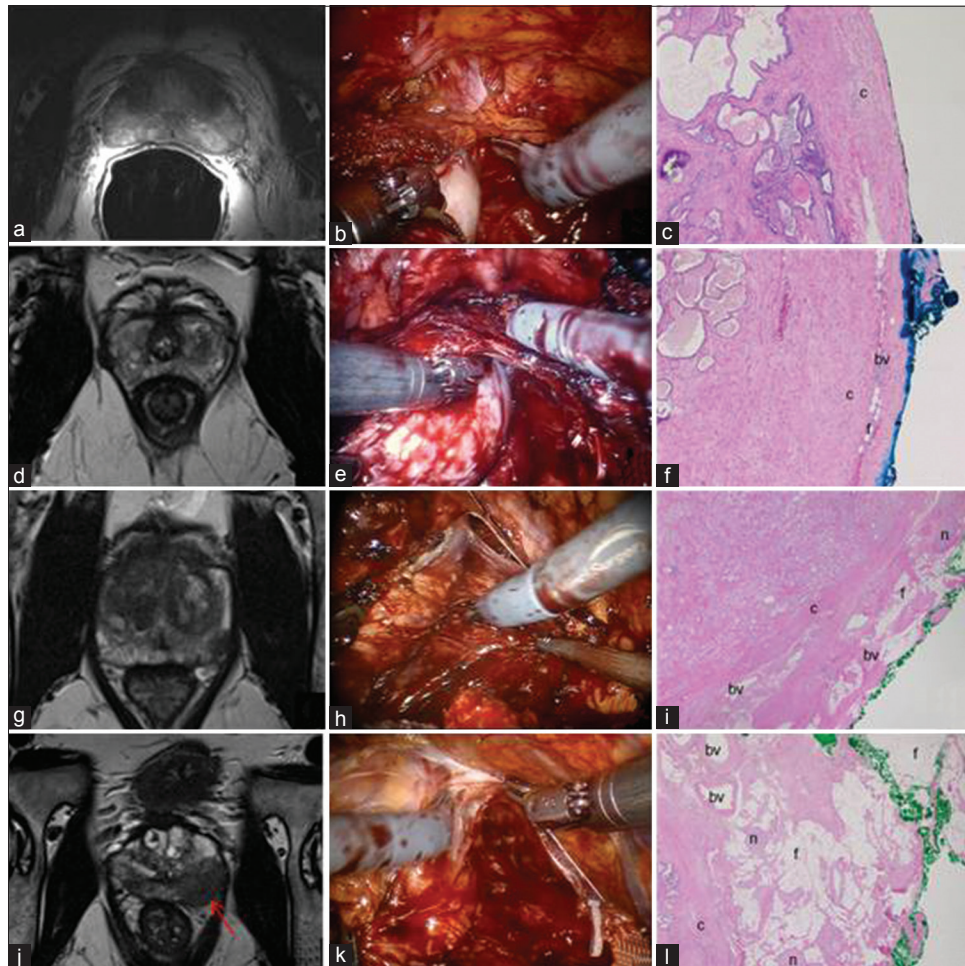


Figure 4: Pre-operative multiparametric magnetic resonance imaging in risk stratification and intraoperative planning for graded nerve spare, intraoperative views and corresponding histology from the edge for Grade 1 (a,b,c), Grade 2 (d, e, f), Grade 3 (g, h, i) and Grade 4 (j, k, l) nerve spare. (c – capsule; bv – blood vessel; f – periprostatic fat; n – nerve bundle). The red arrow in J points to the site of extracapsular extension

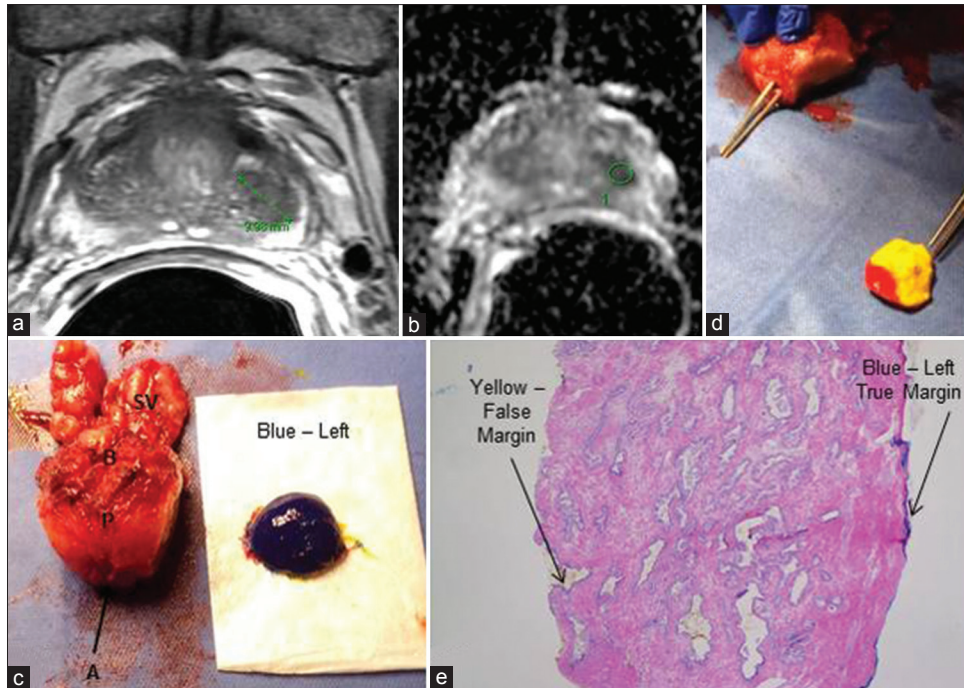


Figure 5: Magnetic resonance imaging (MRI)-guided intraoperative frozen section. (a) T2-weighted MRI and (b) diffusion-weighted imaging (DWI) demonstrating a left-sided lesion (marked in green). (c,d) A radical prostatectomy specimen (P) with left lateral margin transected for intraoperative frozen section (left true margin marked in blue, false left margin in yellow inked as red at the apex). (e) Intraoperative frozen section from the left margin (blue and yellow represent true and false margins, respectively). (B = base; A = apex; SV = seminal vesicles)

to maintain the delicate balance between oncological control and preserving functional outcomes, it is crucial for the surgeon to be able to identify and better define the NVB in relation to the prostate in real-time. Optical magnification with surgical loupes, intraoperative nerve stimulation and real-time robotic transrectal ultrasound (TRUS Robot) have been attempted.

Diffusion tensor magnetic resonance imaging (DTI)
 DTI is an emerging technology to facilitate treatment planning. It is based on the sensitivity of the water protons measured in the microstructural environment.^[34] The main quantitative measurements of DTI include average diffusivity and fractional anisotropy.^[35] DTI, currently used for neuroimaging applications, enables tracing of the periprostatic nerves. Its utility in human prostates was first reported by Sinha in 2004.^[36] In a recent study using DTI along with mp MRI, the authors demonstrated that of DTI, 2D-T2-weighted MRI and 3D-T2-weighted MRI, only DTI fiber tracking allowed assessment of the entire periprostatic nervous plexus and of all the fibers bilaterally at all levels in all the 33 patients included in the study. The authors concluded that this information could be useful for guiding proper NS surgery using an intrafascial or extrafascial robotic approach^[37] or even the graded NS approach, thereby ensuring recovery of erectile function after RP. Figure 6 depicts the fiber tracts from an *ex vivo* robotic radical prostatectomy specimen using high-resolution DTI. DTI seems to have a promising role in the future for NVB preservation during RP.

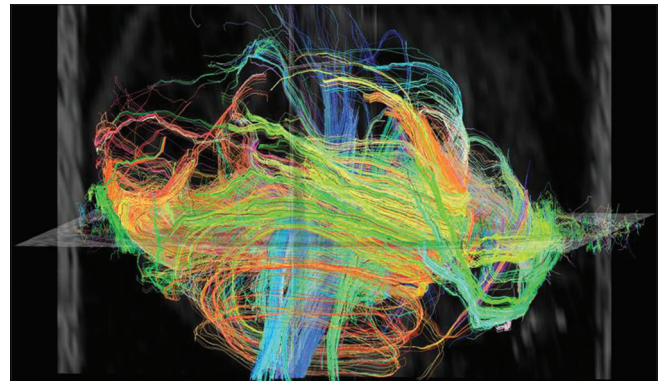


Figure 6: *Ex vivo* diffusion tensor magnetic resonance imaging obtained from robotic radical prostatectomy specimen. The various colors represent the fibers in and around the prostate

Multi-photon microscopy (MPM)

Access to high-resolution real-time imaging of the prostatic capsule, apex, sphincter and the surrounding neurovascular structures is likely to improve oncological and functional outcomes. MPM is one such novel optical imaging technology that relies on the simultaneous absorption of two or three low-energy (near-infrared) photons to cause a non-linear excitation, which reduces the potential for cellular damage.^[38] By adopting a stepwise approach for imaging, researchers were able to identify the cavernous nerve, major pelvic ganglion, prostatic capsule, prostatic acini, fat, vessels and pathological changes in rat models and *ex vivo* human prostatectomy specimens^[38,39] [Figure 7]. “Real-time tissue imaging”

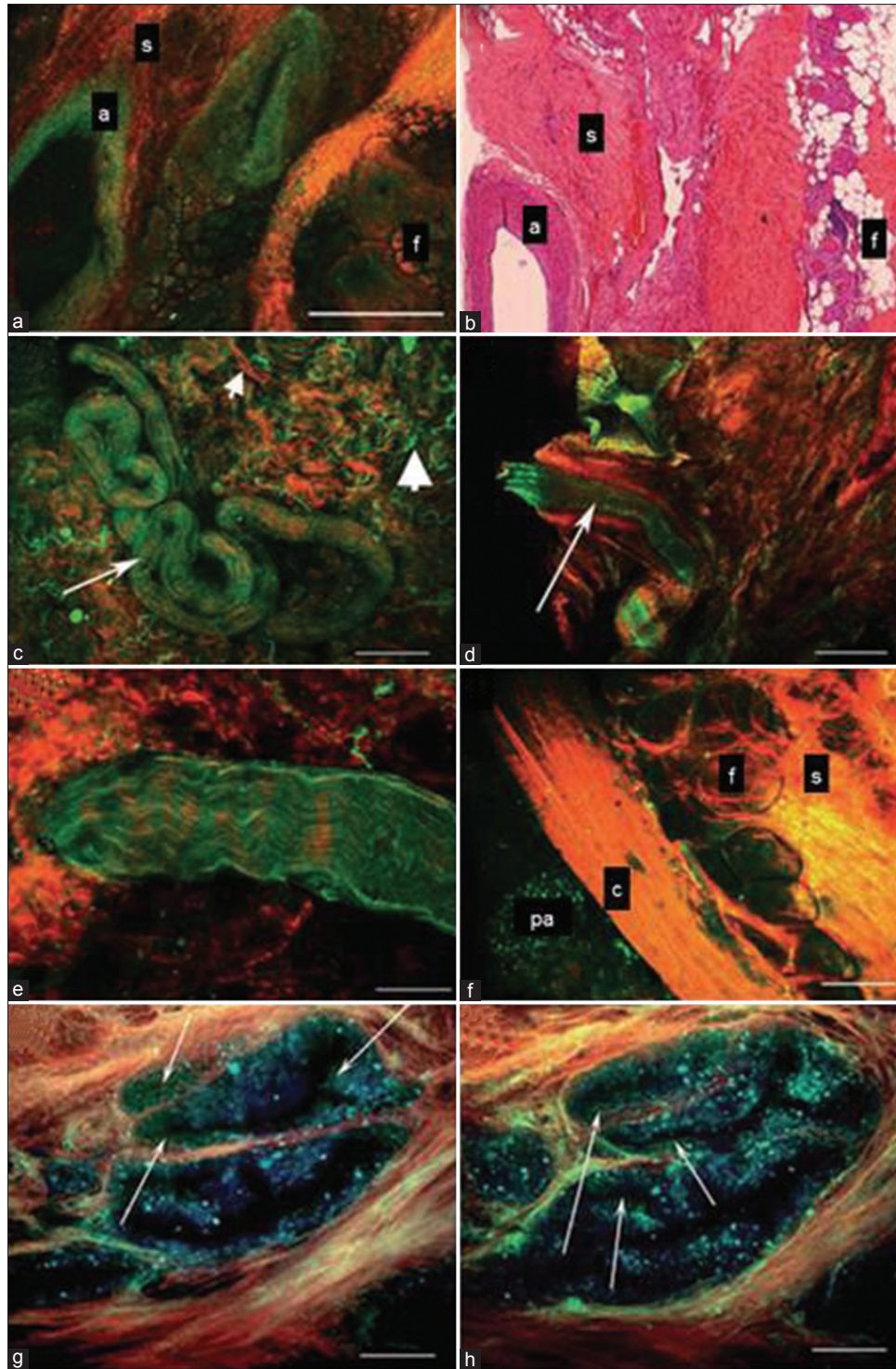


Figure 7: Multi-photon microscopy (MPM) images from ex vivo human prostate. (a,b) Lateral pelvic fascia showing a large artery (a), fibrocollagenous connective tissue stroma (s) and fat (c) on MPM image (A) and histology slide (B). Note the empty lumen of the artery in A and B. (c) Surgical apical margin showing a small nerve (arrow). Small arrowhead points to collagen and the large arrowhead points to elastin in the connective tissue stroma. (d) Surgical apical margin showing a small artery. Note the empty lumen (arrow) as opposed to the wavy nerve fibers in C and E. (e) Higher magnification image of a small nerve bundle at the surgical margin showing fluorescence that derives from the axoplasm or cytoplasm of the Schwann cells. (f) Prostatic capsule showing an underlying prostatic acinus (pa), capsule (c), periprostatic connective tissue (s) and fat (f). (g,h) Higher magnification of prostatic acini imaged using three detector channels. Cells emit mostly in the 420-530 nm range and thus appear green in the color-coding scheme. By contrast, the gland-associated punctate fluorescence (which could represent lipofuscin deposits) emits over a broader wavelength range and thus appears blue in the color-coding scheme (arrows point to bona fide cells with distinct nuclei). Color-coding of MPM images: Red, second harmonic generation (SHG) (355-420 nm); green, short-wavelength autofluorescence (420-530 nm); blue, long-wavelength autofluorescence (530-650 nm). Scale bars: A, C, D, H 500 μ m; E 67 μ m; F, G 100 μ m [Reproduced and edited with permission from 31]

may help surgeons to localize the nerves in relation to the cancerous tissues and potentially identify possible perineural invasion and extraprostatic extension in real time. This would then minimize nerve damage thus enhancing sexual outcomes and reduce the incidence of PSM. Like most technological innovations, MPM imaging will have to face several potential challenges before it can be integrated into real-time applications.

Optical coherence tomography (OCT)

OCT provides real-time, high-resolution, cross-sectional tissue imaging by measuring the back scatter near-infrared radiation. It is non-invasive and the energy utilized does not cause mechanical damage. Given its fiberoptic nature delivery system, portability and low cost, it can readily be integrated into endoscopic/laparoscopic surgical equipment and probes. The drawback, however, is the inadequate resolution quality for tissues >1 mm deep. Using OCT, the cavernous nerve was distinguished as an intense linear structure separate from the adjacent tissues in *in vivo* experiments on Sprague–Dawley rats; however, the discrimination between adjacent prostatic tissues and nerves was not adequate in *ex vivo* human prostatectomy specimens.^[40] In a feasibility study by Dangle *et al.*, in which OCT was used on 100 *ex vivo* human prostatectomy specimens to identify PSM and extraprostatic extension (EPE), the results were compared against the gold standard histopathology. The reported sensitivity and specificity for PSM were 70% and 84%,

respectively, with 33% and 96% positive predictive value (PPV) and negative predictive value (NPV). The sensitivity, specificity, PPV and NPV for EPE and SV invasion (SVI) were 46%, 84%, 50%, 92% and 33%, 97%, 33% and 97%, respectively. This study established the template for the visual OCT characteristics of the prostate, SV and cancerous tissue. With its high NPV, OCT could be useful to rule out PSM, EPE and SVI.^[41] *In vivo* studies are needed to prove its efficacy in real-time imaging intraoperatively. Beuvon *et al.* have recently tested the feasibility of OCT in prostate biopsies for diagnostic purposes and reported a 81% concordance with histopathological findings.^[42] OCT might have a potential role in the future both in the diagnostic and the therapeutic pathways.

Localization by physiological stimulation

A number of nerve mapping technologies have been investigated to aid in localization of periprostatic nerves for augmenting NS during radical prostatectomy. Mapping is usually performed by stimulating a nerve either by optical or by electrical means and then detecting a physiologic response, such as penile tumescence/detumescence, intracavernosal pressure, intraurethral pressure, impedance or an action potential. Examples of such devices include CaverMap,^[43] ProPep, NIMEclipse and optical nerve monitoring. Table 3 describes the currently available nerve stimulation devices.

Table 3: Characteristics of the nerve stimulation devices

Device	Method	Physiologic response measured	Resolution	Response time	Current status
CaverMap (Blue Torch Medical, Rockville, MD, USA) ^[43]	Electrical stimulation using a probe with 8 electrodes spread over 1.2 cm	Tumescence/detumescence detected by a ring placed around the penis	1.5 mm	Minutes	Most widely tested technology for nerve monitoring, conflicting results. FDA approved
ProPep (ProPep Surgical, Austin, TX, USA)	Electrical stimulation delivered by Maryland bipolar forceps	Detection of action potentials by two electrodes placed in the levator ani muscles. Visual confirmation of levator ani contractions also possible	1-5 mm	Milliseconds	FDA approved in 2012. Further studies warranted in exploring its use to improve functional outcomes. Feasibility study in 20 patients
Fixed bipolar electrode ^[44,45]	Bipolar stimulating electrode	Intracavernosal pressure measured by a needle placed in the corpus cavernosum with or without intraurethral pressure measurement by intraurethral balloon	7 mm	30-60 s	
Needle array probe	Electrical stimulation	Real-time intraoperative electrical impedance tomography	NA	Real-time	Validated <i>in vitro</i> and <i>in vivo</i> using rat sciatic nerves. No human studies
Optical nerve stimulation ^[46]	Nerve stimulation using infrared lasers with a 1-mm diameter beam	Intracavernosal pressure	1 mm	30+s	Rat <i>in vivo</i> studies. No human studies
NIM Eclipse ^[47] (MEDTRONIC, Memphis, TN, USA)	Nerve stimulation using ball tip bipolar probe/modified Foley catheter with ring electrodes	Detection of action potential by a modified Foley catheter/ball tip bipolar probe with ring electrodes, Cavernosal engorgement monitored simultaneously using an StO ₂ monitor	1-5 mm	Milliseconds	Feasibility study performed in humans undergoing RALP

NIM = Nerve integrity monitor, FDA = Food and drug administration, RALP=Robotic-assisted laparoscopic prostatectomy

Dye-based visualization

Nerves can be stained using fluorescent dyes and can be identified based on specific characteristics such as the method of delivery, nerve specificity, time for staining and resolution. When applied directly by local infiltration into the base of the penis, these dyes travel via the retrograde transport mechanism along the erectile nerves. Systemic administration of the dye results in labeling of all or most of the nerves, and hence the labeled nerves may not be responsible for erectile function. Local injections have a limited utility as well, as they label only one nerve fiber tract at a time. In addition, axonal transport is a slow process and can take a long time, sometimes up to several months. Currently, indocyanine green and fluorescein are the only FDA-approved dyes that have been studied in RP. Other examples of nerve dyes include compounds from Avelas and General Electric, fluorescent cholera toxin subunit B, indocyanine green, fluorescent-inactivated herpes simplex 2 and Fluoro-Gold.^[48]

Neurovascular bundle reconstruction

Wide excision of the NVBs is a prudent approach followed by most surgeons when there is a high index of suspicion of ECE and NVB invasion by tumor based on pre-operative parameters. However, there is no consensus on the ideal method for NVB reconstruction. While there are a few existing options to choose from, namely sural nerve grafting,^[49] use of embryonic stem cells or growth factors to enhance neural regeneration,^[50] entubulization model of cavernosal nerve^[51] or nerve advancement with end-to-end reconstruction,^[52] none of them are employed routinely.

Nerve advancement technique (NAT) is one such technique based on neuroscientific concepts of peripheral nerve repair that attempts to establish continuity between the proximal and distal nerve stumps by end-to-end anastomosis of the partially resected NVB [Figure 8]. Geuna *et al.* and Terzis *et al.* reported that if continuity is restored by end-to-end suturing, bands of Bungner arise from axons upstream of the point of transection and grow along the glial columns in the distal nerve stump to eventually re-innervate the denervated

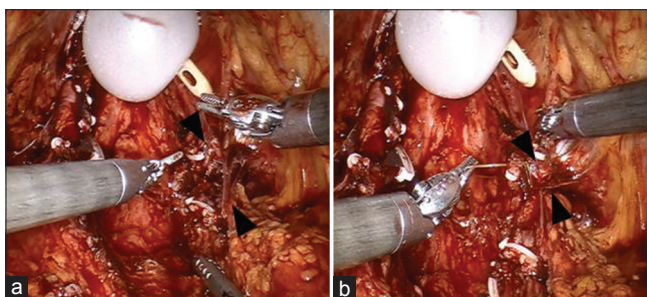


Figure 8: Nerve advancement technique (NAT). (a) Black arrow heads mark the location of partially resected neurovascular bundle. (b) Black arrow heads mark the approximated ends of neurovascular bundles using the nerve advancement technique (NAT)

structures.^[53,54] Tewari *et al.* performed nerve advancement and end-to-end, tension-free anastomosis of the proximal and distal neural stumps following partial resection of NVBs in a pilot study of seven pre-operatively potent, high-risk patients. One patient had a PSM and five of the seven men regained potency. They reported that NAT is technically feasible, oncologically safe and is associated with promising sexual outcomes.^[52]

CONCLUSION

Much of the success achieved in the last decade in terms of improved trifecta outcomes following robotic radical prostatectomy relates to the adoption of an athermal, traction-free, risk-stratified, graded nerve spare approach to preserve the neural hammock. Innovative techniques to incorporate real-time intraoperative imaging and nerve mapping methodologies to identify and preserve the cavernosal nerves seem to have a challenging but promising role in the future.

ACKNOWLEDGMENTS

The authors are thankful to Dr. Bachir Taouli MD, Dr. Cheuk Ying Tang PhD, Dr. Victoria Wang PhD and Dr. Edmund Wong PhD, from the Department of Radiology, Icahn School of Medicine, for providing the *ex vivo* image for diffusion tensor imaging.

REFERENCES

1. Noldus J, Graefen M, Haese A, Henke RP, Hammerer P, Huland H. Stage migration in clinically localized prostate cancer. *Eur Urol* 2000;38:74-8
2. Magheli A, Burnett AL. Erectile dysfunction following prostatectomy: Prevention and treatment. *Nat Rev Urol* 2009;6:415-27.
3. Ficarra V, Novara G, Rosen RC, Artibani W, Carroll PR, Costello A, *et al.* Systematic review and meta-analysis of studies reporting urinary continence recovery after robot-assisted radical prostatectomy. *Eur Urol* 2012;62:405-17.
4. Trinh QD, Sammon J, Sun M, Ravi P, Ghani KR, Bianchi M, *et al.* Perioperative outcomes of robot-assisted radical prostatectomy compared with open radical prostatectomy: Results from the nationwide inpatient sample. *Eur Urol* 2012;61:679-85.
5. Tewari A, Sooriakumaran P, Bloch DA, Seshadri-Kreaden U, Hebert AE, Wiklund P. Positive surgical margin and perioperative complication rates of primary surgical treatments for prostate cancer: A systematic review and meta-analysis comparing retropubic, laparoscopic, and robotic prostatectomy. *Eur Urol* 2012;62:1-15.
6. Choi WW, Freire MP, Soukup JR, Yin L, Lipsitz SR, Carvas F, *et al.* Nerve-sparing technique and urinary control after robot-assisted laparoscopic prostatectomy. *World J Urol* 2011;29:21-7.
7. Sammon JD, Sharma P, Trinh QD, Ghani KR, Sukumar S, Menon M. Predictors of immediate continence following robot-assisted radical prostatectomy. *J Endourol* 2013;27:442-6.
8. Walsh P. Impotence following radical prostatectomy: Insight into etiology and prevention. *J Urol* 1982;128:492-7.
9. Tewari A, Peabody JO, Fischer M, Sarle R, Vallancien G, Delmas V, *et al.* An operative and anatomic study to help in nerve sparing during laparoscopic and robotic radical prostatectomy. *Eur Urol* 2003;43:444-54.

10. Menon M, Tewari A, Peabody J. Vattikuti Institute prostatectomy: Technique. *J Urol* 2003;169:2289-92.
11. Savera AT, Kaul S, Badani K, Stark AT, Shah NL, Menon M. Robotic radical prostatectomy with the "Veil of Aphrodite" technique: Histologic evidence of enhanced nerve sparing. *Eur Urol* 2006;49:1065-74.
12. Tewari A, Takenaka A, Mtui E, Horninger W, Peschel R, Bartsch G, *et al.* The proximal neurovascular plate and the trizonal neural architecture around the prostate gland: Importance in the athermal robotic technique of nerve sparing prostatectomy. *BJU Int* 2006;98:314-23.
13. Takenaka A, Leung RA, Fujisawa M, Tewari AK. Anatomy of autonomic nerve component in the male pelvis: The new concept from a perspective for robotic nerve sparing radical prostatectomy. *World J Urol* 2006;24:136-43.
14. Takenaka A, Kawada M, Murakami G, Hisasue S, Tsukamoto T, Fujisawa M. Interindividual variation in distribution of extramural ganglion cells in the male pelvis: A semi-quantitative and immunohistochemical study concerning nerve-sparing pelvic surgery. *Eur Urol* 2005;48:46-52.
15. Costello AJ, Brooks M, Cole OJ. Anatomical studies of the neurovascular bundle and cavernosal nerves. *BJU Int* 2004;94:1071-6.
16. Eichelberg C, Erbersdobler A, Michl U, Schlomm T, Salomon G, Graefen M, *et al.* Nerve distribution along the prostatic capsule. *Eur Urol* 2007;51:105-11.
17. Kaul S, Bhandari A, Hemal A, Savera A, Shrivastava A, Menon M. Robotic radical prostatectomy with preservation of the prostatic fascia: A feasibility study. *Urology* 2005;66:1261-5.
18. Menon M, Shrivastava A, Bhandari M, Satyanarayana R, Siva S, Agarwal PK. Vattikuti Institute prostatectomy: Technical modifications in 2009. *Eur Urol* 2009;56:89-96.
19. Tewari A, El-Hakim A, Horninger W, Peschel R, Coll D, Bartsch G. Nerve-sparing during robotic radical prostatectomy: Use of computer modeling and anatomic data to establish critical steps and maneuvers. *Curr Urol Rep* 2005;6:126-8.
20. Leung RA, Kim TS, Tewari AK. Future directions of robotic surgery: A case study of the Cornell athermal robotic technique of prostatectomy. *Sci World J* 2006;6:2553-9.
21. El-Hakim A, Leung RA, Richstone L, Kim TS, Te AE, Tewari AK. Athermal Robotic Technique of prostatectomy in patients with large prostate glands (> 75 g): Technique and initial results. *BJU Int* 2006;98:47-9.
22. Tewari A, Rao S, Martinez-Salamanca JI, Leung R, Ramanathan R, Mandhani A, *et al.* Cancer control and the preservation of neurovascular tissue: How to meet competing goals during robotic radical prostatectomy. *BJU Int* 2008;101:1013-8.
23. Ahlering TE, Rodriguez E, Skarecky DW. Overcoming obstacles: Nerve-sparing issues in radical prostatectomy. *J Endourol* 2008;22:745-50.
24. Ficarra V, Novara G, Ahlering TE, Costello A, Eastham JA, Graefen M, *et al.* Systematic review and meta-analysis of studies reporting potency rates after robot-assisted radical prostatectomy. *Eur Urol* 2012;62:418-30.
25. Breza J, Aboseif S, Orvis B, Lue T, Tanagho E. Detailed anatomy of penile neurovascular structures: Surgical significance. *J Urol* 1989;141:437-43.
26. Tewari A, Srivastava A, Sooriakumaran P, Grover S, Dorsey P, Leung R. Technique of traction-free nerve-sparing robotic prostatectomy: Delicate tissue handling by real-time penile oxygen monitoring. *Int J Impot Res* 2012;24:11-9.
27. Jhaveri JC, Te A, Takenaka A, Tu J, Yadav R, Rao S, *et al.* Grades of robotic nerve sparing. Award Winning Video. AUA 2008. Available from: <http://www.vimeo.com/6599375>. [Last accessed on 2014 Sep 09].
28. Tewari AK, Patel ND, Leung RA, Yadav R, Vaughan ED, El-Douaihy Y, *et al.* Visual cues as a surrogate for tactile feedback during robotic-assisted laparoscopic prostatectomy: Posterolateral margin rates in 1340 consecutive patients. *BJU Int* 2010;106:528-36.
29. Srivastava A, Grover S, Sooriakumaran P, Tan G, Takenaka A, Tewari AK. Neuroanatomic basis for traction-free preservation of the neural hammock during athermal robotic radical prostatectomy. *Curr Opin Urol* 2011;21:49-59.
30. Tewari AK, Srivastava A, Huang MW, Robinson BD, Shevchuk MM, Durand M, *et al.* Anatomical grades of nerve sparing: A risk-stratified approach to neural-hammock sparing during robot-assisted radical prostatectomy (RARP). *BJU Int* 2011;108:984-92.
31. Schatloff O, Chauhan S, Kameh D, Valero R, Ko YH, Sivaraman A, *et al.* Cavernosal nerve preservation during robot-assisted radical prostatectomy is a graded rather than an all-or-none phenomenon: Objective demonstration by assessment of residual nerve tissue on surgical specimens. *Urology* 2012;79:596-600.
32. Moskovic DJ, Alphas H, Nelson CJ, Rabbani F, Eastham J, Touijer K, *et al.* Subjective characterization of nerve sparing predicts recovery of erectile function after radical prostatectomy: Defining the utility of a nerve sparing grading system. *J Sex Med* 2011;8:255-60.
33. Schlomm T, Tennstedt P, Huxhold C, Steuber T, Salomon G, Michl U, *et al.* Neurovascular structure-adjacent frozen-section examination (NeuroSAFE) increases nerve-sparing frequency and reduces positive surgical margins in open and robot-assisted laparoscopic radical prostatectomy: Experience after 11,069 consecutive patients. *Eur Urol* 2012;62:333-40.
34. Farrell JA, Landman BA, Jones CK, Smith SA, Prince JL, van Zijl PC, *et al.* Effects of signal-to-noise ratio on the accuracy and reproducibility of diffusion tensor imaging-derived fractional anisotropy, mean diffusivity, and principal eigenvector measurements at 1.5 T. *J Magn Reson Imaging* 2007;26:756-67.
35. Tan N, Margolis DJ, McClure TD, Thomas A, Finley DS, Reiter RE, *et al.* Radical prostatectomy: Value of prostate MRI in surgical planning. *Abdom Imaging* 2012;37:664-74.
36. Sinha S, Sinha U. *In vivo* diffusion tensor imaging of the human prostate. *Magn Reson Med* 2004;52:530-7.
37. Panebianco V, Barchetti F, Sciarra A, Marcantonio A, Zini C, Salciccia S, *et al.* *In vivo* 3D neuroanatomical evaluation of periprostatic nerve plexus with 3T-MR Diffusion Tensor Imaging. *Eur J Radiol* 2013;82:1677-82.
38. Tewari AK, Shevchuk MM, Sterling J, Grover S, Herman M, Yadav R, *et al.* Multiphoton microscopy for structure identification in human prostate and periprostatic tissue: Implications in prostate cancer surgery. *BJU Int* 2011;108:1421-9.
39. Yadav R, Mukherjee S, Hermen M, Tan G, Maxfield FR, Webb WW, *et al.* Multiphoton microscopy of prostate and periprostatic neural tissue: A promising imaging technique for improving nerve-sparing prostatectomy. *J Endourol* 2009;23:861-7.
40. Fried NM, Rais-Bahrami S, Lagoda GA, Chuang Y, Burnett AL, Su LM. Imaging the cavernous nerves in the rat prostate using optical coherence tomography. *Lasers Surg Med* 2007;39:36-41.
41. Dangle PP, Shah KK, Kaffenberger B, Patel VR. The use of high resolution optical coherence tomography to evaluate robotic radical prostatectomy specimens. *Int Braz J Urol* 2009;35:344-53.
42. Beuvon F, Dalimier E, Cornud F, Barry DN. Full field optical coherence tomography of prostate biopsies: A step towards pre-histological diagnosis? Article in French. *Prog Urol* 2014;24:22-30.
43. Klotz L. Cavernosal nerve mapping: Current data and applications. *BJU Int* 2004;93:9-13.
44. Kurokawa K, Suzuki T, Suzuki K, Terada N, Ito K, Yoshikawa D, *et al.* Preliminary results of a monitoring system to confirm the preservation of cavernous nerves. *Int J Urol* 2003;10:136-40.
45. Kurokawa K, Suzuki T, Suzuki K, Ito K, Shimizu N, Fukabori Y. A simple and reliable monitoring system to confirm the preservation of the cavernous nerves. *Int J Urol* 2001;8:231-6.
46. Fried NM, Lagoda GA, Scott NJ, Su LM, Burnett AL. Noncontact stimulation of the cavernous nerves in the rat prostate using a tunable-wavelength thulium fiber laser. *J Endourol* 2008;22:409-13.

47. Tewari A, Badani K, Singhal P, Ali A, Leung R, Antonucci B, *et al.* V5-05. Intraoperative periprostatic nerve action potential monitoring during robotic prostatectomy. *J Urol* 2014 01/04/2014:191.
48. Ponnusamy K, Sorger JM, Mohr C. Nerve mapping for prostatectomies: Novel technologies under development. *J Endourol* 2012;26:769-77.
49. Kim ED, Scardino PT, Hampel O, Mills NL, Wheeler TM, Nath RK. Interposition of sural nerve restores function of cavernous nerves resected during radical prostatectomy. *J Urol* 1999;161:188-92.
50. Bochinski D, Lin GT, Nunes L, Carrion R, Rahman N, Lin CS, *et al.* The effect of neural embryonic stem cell therapy in a rat model of cavernosal nerve injury. *BJU Int* 2004;94:904-9.
51. Ball RA, Lipton SA, Dreyer EB, Richie JP, Vickers MA. Entubulization repair of severed cavernous nerves in the rat resulting in return of erectile function. *J Urol* 1992;148:211-5.
52. Martinez-Salamanca JI, Rao S, Ramanathan R, Gonzalez J, Mandhani A, Yang X, *et al.* Nerve advancement with end-to-end reconstruction after partial neurovascular bundle resection: A feasibility study. *J Endourol* 2007;21:830-5.
53. Geuna S, Papalia I, Tos P. End-to-side (terminolateral) nerve regeneration: A challenge for neuroscientists coming from an intriguing nerve repair concept. *Brain Res Rev* 2006;52:381-8.
54. Terzis JK, Sun DD, Thanos PK. Historical and basic science review: Past, present, and future of nerve repair. *J Reconstr Microsurg* 1997;13:215-25.

How to cite this article: Pisipati S, Ali A, Mandalapu RS, Haines GK, Singhal P, Reddy BN, *et al.* Newer concepts in neural anatomy and neurovascular preservation in robotic radical prostatectomy. *Indian J Urol* 2014;30:399-409.

Source of Support: Nil, **Conflict of Interest:** Dr. Ashutosh Tewari discloses that he is the principal investigator on research grants from Intuitive Surgical, Inc. (Sunnyvale, CA, USA) and Boston Scientific Corporation; he is a non-compensated director of the Prostate Cancer Institute (Pune, India) and Global Prostate Cancer Research Foundation; he has received research funding from the Prostate Cancer Foundation, The LeFrak Family Foundation, Mr. and Mrs. Paul Kanavos, Craig Efron & Company, Charles Evans Foundation and Christian and Heidi Lange Family Foundation. Dr. Sailaja Pisipati and Dr. Adnan Ali are recipients of the Prostate Cancer Foundation Young Investigator Award.

Author Help: Online submission of the manuscripts

Articles can be submitted online from <http://www.journalonweb.com>. For online submission, the articles should be prepared in two files (first page file and article file). Images should be submitted separately.

1) **First Page File:**

Prepare the title page, covering letter, acknowledgement etc. using a word processor program. All information related to your identity should be included here. Use text/rtf/doc/pdf files. Do not zip the files.

2) **Article File:**

The main text of the article, beginning with the Abstract to References (including tables) should be in this file. Do not include any information (such as acknowledgement, your names in page headers etc.) in this file. Use text/rtf/doc/pdf files. Do not zip the files. Limit the file size to 1 MB. Do not incorporate images in the file. If file size is large, graphs can be submitted separately as images, without their being incorporated in the article file. This will reduce the size of the file.

3) **Images:**

Submit good quality color images. Each image should be less than 4096 kb (4 MB) in size. The size of the image can be reduced by decreasing the actual height and width of the images (keep up to about 6 inches and up to about 1800 x 1200 pixels). JPEG is the most suitable file format. The image quality should be good enough to judge the scientific value of the image. For the purpose of printing, always retain a good quality, high resolution image. This high resolution image should be sent to the editorial office at the time of sending a revised article.

4) **Legends:**

Legends for the figures/images should be included at the end of the article file.